




Economic Approach for Synthesis of Gold Nanoparticle-based Freeze Indicator for Fish Products

Sreelakshmi K. R. , Mohan C. O. and Renjith R. K.

ICAR-Central Institute of Fisheries Technology, Matsyapuri, Cochin, Kerala (682 029), India



Corresponding  sreecift@gmail.com

 0000-0001-5421-9065

ABSTRACT

This study was conducted during the period September 2020–January 2023 at ICAR-Central Institute of Fisheries Technology, Cochin. The study was to develop a cost-effective freeze indicator using gold nanoparticles. Gold nanoparticles (AuNPs) were synthesized using chitosan and trisodium citrate (TSC) as a reducing agent. Various chitosan samples with different molecular weights were obtained from commercial chitosan units. Chitosan was employed at two distinct concentrations. The UV-Vis spectra exhibited the characteristic peak of AuNPs at 520–530 nm in all analyzed samples. The samples containing chitosan displayed a light pink color, whereas those containing TSC exhibited a ruby red color. An increase in chitosan concentration led to an increase in absorbance of the SPR peak. The full width at half maximum (FWHM), zeta potential, and conductivity of the nanoparticles were also investigated. The stability of the synthesized nanoparticles was assessed during frozen storage at -18°C , revealing that the sample containing TSC became colorless upon freezing. The stability of chitosan-containing samples improved with higher concentrations and molecular weights. No distinct color change upon freezing was observed in the samples synthesized using chitosan. The AuNPs synthesized using TSC were evaluated and the significant color change demonstrated by the sample confirmed that the nanoparticle solution synthesized using TSC at a gold concentration of 1 mM can serve as an effective freeze indicator for food and pharmaceutical applications.

KEYWORDS: Chitosan, colour, freezing, gold nanoparticles, trisodium citrate

Citation (VANCOUVER): Sreelakshmi et al., Economic Approach for Synthesis of Gold Nanoparticle-based Freeze Indicator for Fish Products. *International Journal of Bio-resource and Stress Management*, 2024; 15(4), 01-08. [HTTPS://DOI.ORG/10.23910/1.2024.5153](https://doi.org/10.23910/1.2024.5153).

Copyright: © 2024 Sreelakshmi et al. This is an open access article that permits unrestricted use, distribution and reproduction in any medium after the author(s) and source are credited.

Data Availability Statement: Legal restrictions are imposed on the public sharing of raw data. However, authors have full right to transfer or share the data in raw form upon request subject to either meeting the conditions of the original consents and the original research study. Further, access of data needs to meet whether the user complies with the ethical and legal obligations as data controllers to allow for secondary use of the data outside of the original study.

Conflict of interests: The authors have declared that no conflict of interest exists.

RECEIVED on 18th January 2024 RECEIVED in revised form on 17th March 2024 ACCEPTED in final form on 10th April 2024 PUBLISHED on 19th April 2024



1. INTRODUCTION

Chitin constitutes about 50–80% of the organic compounds in crustacean shells and cuticles of insects (Li et al., 2020). The shell fish processing industry generates a huge amount of waste which is mainly constituted by the shell of animals. Chitosan mainly consists of β -(1–4)-linked 2-acetamido-2-deoxy- β -D-glucopyranose and 2-amino-2-deoxy- β -D-glycopyranose which functions as structural polysaccharide (Tyagi et al., 1996). The specific properties of chitosan like molecular weight and degree of deacetylation depends on processing conditions like strength of chemical used for demineralisation and deacetylation, the temperature conditions and atmospheric conditions. It is non-toxic, biodegradable, biocompatible and have antioxidant properties (Osman and Arof, 2003).

The commercial applications of chitin and chitosan mainly arises due to the high percentage of nitrogen (6–89%) compared to cellulose (1.25%). The nitrogen content of chitin varies from 5% to 8% which depends on the degree of deacetylation and in chitosan the presence of nitrogen is mainly in the form of primary aliphatic amino groups (Ravikumar, 1999). Chitosan has a positive ionic charge and can chemically bind with negatively charged compounds like fats and bile acids (Sandford et al., 1992). Over the last decade, chitosan which is one of the promising polymeric materials is used extensively for pharmaceuticals and biomedical industries. (Prashanth and Taranathan, 2007).

Metal nanoparticles have a wide range of applications because of their unique properties (Sun et al., 2017). Gold nanoparticles are inert and have bactericidal effect on pathogens. The pharmacological applications include drug delivery, tumor destruction, gene delivery, food industry, separation science, pharmacokinetic studies, health care, drug delivery, gene delivery, optics and space industry (Santhoshkumar et al., 2017). The synthesis of gold nanoparticles requires a reducing agent for converting the gold ions to nanoparticles. Several chemicals like ascorbic acid (Merza et al., 2012), potassium bitartrate and sodium citrate (Kinling et al., 2006) are efficiently used for synthesis of gold nanoparticles. These chemicals are either toxic, expensive or aggressive in nature. So alternative methods of synthesis that are eco-friendly and economical are to be explored. The effectiveness of the preparation using these alternative methods depends on the reducing agent, the stabilising agent and the solvent used (Sun et al., 2008). The reducing and stabilising agent determines the size and shape of AuNPs formed.

Plant and animal products mediated synthesis of nanoparticles gains attention as these derivatives can act as both reducing and capping agent for nanoparticles (Harikrishnan et al., 2022, Najlaa et al., 2022, Kamaraj et al., 2022, Khan et

al., 2022, Mihir et al., 2021). Of these, chitosan is gaining wide importance and the glucosamine units will exist in open chain forms at the end of chitosan chains and the oxidation of these groups helps in nanoparticle formation. The properties of chitosan affects the properties of AuNPs formed also. Several authors have reported the synthesis of nanoparticles using chitosan (Amr et al., 2022, Gao et al., 2024, Sreelakshmi et al. 2021a, Sreelakshmi et al. 2021b, Dananjaya et al. 2017). The development of gold nanoparticles using chitosan and its freezing were studied by Mohan et al. (2019) and Sreelakshmi et al. (2022a). The commercial production of chitosan results in different characteristics like degree of deacetylation, molecular weight, viscosity etc. These characteristics have indeed substantial effect on the performance of chitosan (Sreelakshmi et al., 2022b) and the performance of gold nanoparticles as freeze indicator using 10 mM gold precursor. The use of gold precursor is to be reduced to make the technology more economical. The present study was undertaken to explore the possibility of developing a cost effective freeze indicator using gold nanoparticles by a lower concentration of gold concentration. For this using two different methods of synthesis, Turkevich and green synthesis were compared.

2. MATERIALS AND METHODS

2.1. Materials

Different chitosan samples (chitosan 1 with molecular weight 2387 KDa, chitosan 2 with MW 1724 KDa and chitosan 3 with MW 743 KDa) extracted from shrimp processing waste were purchased from a chitosan manufacturing company, India Seafoods Pvt. Ltd. at Cochin, Kerala, India. The chitosan 4 with MW 685 KDa was purchased from Sigma-Aldrich, USA. The chitosan samples had almost similar degree of deacetylation of 80%–85%. The hydrogen tetrachloroaurate (III) trihydrate was purchased from Himedia, Mumbai, India and other chemicals were obtained from Merck Life Science Ltd., India.

2.2. Preparation of AuNPs

All the chitosan samples were dissolved in 1% acetic acid (w/v) separately. The concentration of chitosan used was 0.1% and 0.5%. To this 5 ml gold precursor solution (1mM) was added and heating at 90°C was given continuously. Heating was done for 5 minutes and was cooled and kept in refrigerator. In order to compare the chitosan capped gold nanoparticles with traditional way of chemical synthesis, gold precursor was heated to boiling and trisodium citrate (5 ml) was added to the solution and was heated for 5 minutes. All the samples were studied for UV-Visible spectra, Z-potential, particle size and visible colour.

2.3. Zeta potential

The zeta potential, which determines the surface charge



of nanoparticles was determined using the Zetasizer nanoseries (Malvern Instruments, UK). This is based on photon correlation microscopy. The average zeta potential was determined in milli Volts.

2.4. UV-Visible spectra

The absorption spectra of gold nanoparticles was monitored using Jasco Dual Beam Spectrophotometer (Model V-570, Jasco International Pvt Ltd., Japan). The wavelength of measurement was 400-700nm (Wang et al., 2017). The FWHM was calculated from the spectral data (Keijok et al., 2019).

2.5. Stability of AuNPs on freezing

The gold nanoparticles synthesised were studied for the stability on frozen storage. A known volume of the samples were exposed to frozen temperature (-18±2°C) for 96hrs and the changes were monitored using UV-Vis spectra at 400-700 nm and visible colour changes. The analysis was done after thawing the frozen samples for one hour at room temperature.

2.6. Statistical analysis

The effect of two independent variables on 5 dependent variables were studied using the response contour plots analysed using SAS version 9.2.

3. RESULTS AND DISCUSSION

The pure chitosan solution was colourless and on heating the gold precursor, the colour changed to light yellow. On continuous heating the colour changed to light pink and the treatment was given for 5 minutes with continuous stirring at 500rpm (Figure 1). The formation of pink colour is due to the synthesis of gold nanoparticles on reduction of Au³⁺ ions. There are three steps in formation of gold nanoparticles using chitosan (Sun et al., 2017). First includes the electrostatic interaction of protonated NH₂ groups at second carbon atom of chitosan and gold chloride ions. The second step is the oxidation of C-1 and C-6 carbon atoms in chitosan with reduction of gold ions. Third step

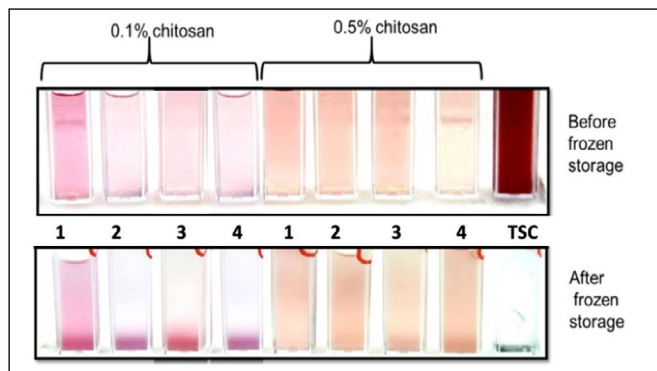


Figure 1: The colour of AuNPs synthesised and the colour change on freezing

includes the columbic interactions and covalent bonding of gold hydroxychlorides with the support. The addition of heat energy facilitates the formation of nanoparticles (Akthar et al., 2013). The sample synthesised with TSC have changed the colour from light pink to ruby red by the end of treatment.

The surface plasmonic resonance, which is attributed by the collective oscillation of electrons at the surface of nanoparticles gives the colour of the nanoparticle solutions²⁰. The characteristic surface plasmonic resonance peak of AuNPs gives bands around 520nm²¹. The peak position, intensity and band width of the spectra depends on the productivity, shape and size of nanoparticles (Regiel-Futyrta et al., 2015). The UV-Vis spectra of AuNPs are given in Figure 2 and 3. The synthesised chitosan-gold nanocomposites have a single absorption spectrum. It was seen that all the chitosan samples were able to reduce gold chloride and SPR peak was observed ~530 nm. The absorbance of SPR (A_{max}, Table 1) increased with the increased concentration of chitosan indicating the higher productivity of AuNPs, except for chitosan 1. Chitosan 1

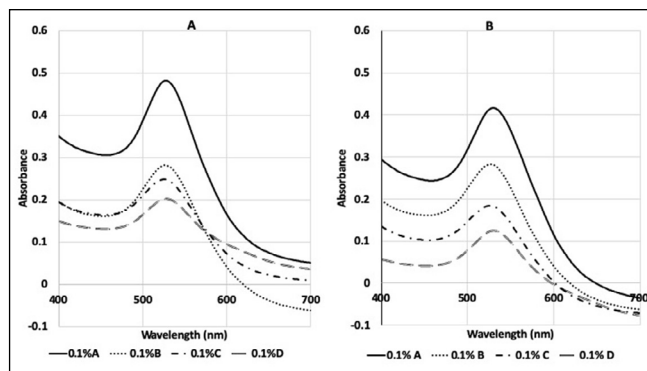


Figure 2: The UV-Vis spectra of nanoparticles synthesised with 0.1% chitosan after freezing. A) before freezing B) after freezing. In legends, A represents chitosan 1, B chitosan 2, C chitosan 3 and D is chitosan 4

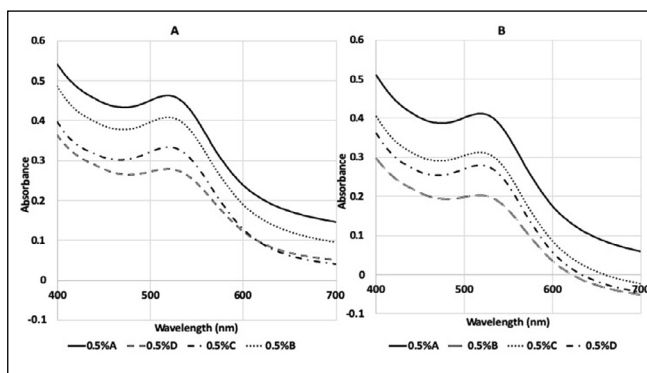


Figure 3: The UV-Vis spectra of nanoparticles synthesised with 0.5% chitosan after freezing. A) before freezing B) after freezing. In legends, A represents chitosan 1, B chitosan 2, C chitosan 3 and D is chitosan 4

is having the higher molecular weight and on increase of concentration, the intermolecular forces within the chitosan chain increases and hence intensity decreases. At specific concentration, the intensity of nanoparticles increased with increase in molecular weight. The λ_{\max} of the samples have also changed with concentration. The peak of the spectra appeared in the lower wavelength when the concentration increased in all the samples. The spectra of AuNP synthesised using TSC is given in figure 4. The absorption spectra have a peak at 526nm with an absorption maxima of 2.84. This high intensity of spectra can be correlated to the intense colour of the sample.

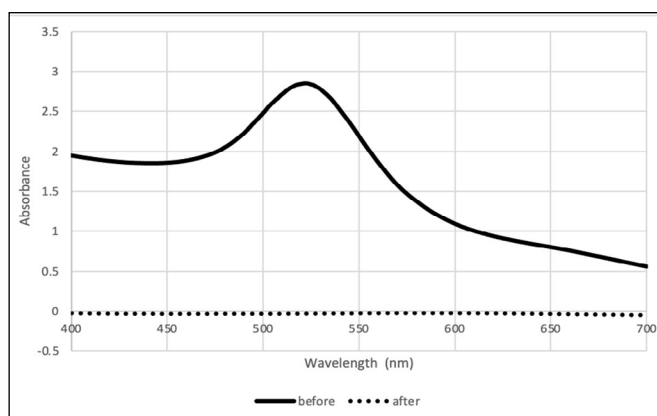


Figure 4: Colour change of AuNPs synthesised with TSC before and after freezing

The full width at half maximum (Table 1) of the samples have increased with increase in concentration of the samples. The absorbance peak becomes broadened in samples synthesised with 0.5% chitosan. This shows that the AuNPs became polydisperse as the higher values of FWHM is an index of higher polydispersity. The AuNPs synthesised with TSC have lesser FWHM than most of the other samples and this shows that the particle size variation of the nanoparticles formed is lesser than that with chitosan. Zeta potential is

the measurement used for assessing the stability of aqueous dispersions in colloidal state. The zeta potential of gold nanoparticles are shown in Table 1. The higher the charge of nanoparticles, the higher will be the electrostatic repulsion and thus lower will be the aggregation of particles. The zeta potential measurement revealed that the zeta potential of the samples increased with increase in concentration of chitosan. The AuNPs synthesised using chitosan had higher charges than the one with TSC which exhibited negative magnitude. In all samples the zeta potential increased with decrease in molecular weight. Electrical conductivity is important in many device applications involving AuNPs. The conductivity of the solution increases with increase in concentration of gold nanoparticles. In this study the higher concentration of chitosan resulted in higher conductivity of the nanocomposites. The sample synthesised with TSC have lesser conductivity than the samples with chitosan. The conductivity of nanoparticle in solution depends on the dissociation of ions from the nanoparticle surface (Zhang et al., 2005).

3.1. Response contour plots

The methodology applied exclusively to examine the relationship between independent and dependent variables is response surface or response contour. The effect of molecular weight and the concentration of chitosan on synthesis of gold nanoparticles with 0.1mM gold chloride is given in figures 5–9. The maximum absorbance increases with increase in molecular weight at lower chitosan concentrations. As the concentration of chitosan increases, the maximum absorbance reduces and the effect of molecular weight will get nullified. The absorbance peak have higher wavelength of maximum absorbance when the molecular weight of chitosan used is high. At lower chitosan concentration, the molecular weight has no effect on the FWHM and at higher concentrations, the FWHM increases and hence concentration of chitosan

Table 1: Characteristics of AuNPs synthesised using different chitosan

Chitosan	Concentration of chitosan (%)	λ_{\max} (nm)	A_{\max}	FWHM	Zeta potential (mV)	Conductivity (mS/cm)
1	0.1	529-531	0.482	62	36.3	0.823
2	0.1	527	0.276	50	38.2	0.836
3	0.1	524-528	0.248	72	41.9	0.759
4	0.1	524	0.202	65	43.7	0.834
1	0.5	515-521	0.464	80	46.1	1.3
2	0.5	524	0.408	83	40.5	1.35
3	0.5	514-521	0.333	80	45.1	1.23
4	0.5	524	0.279	87	51.2	1.49
TSC		526	2.84	56	-26	0.785

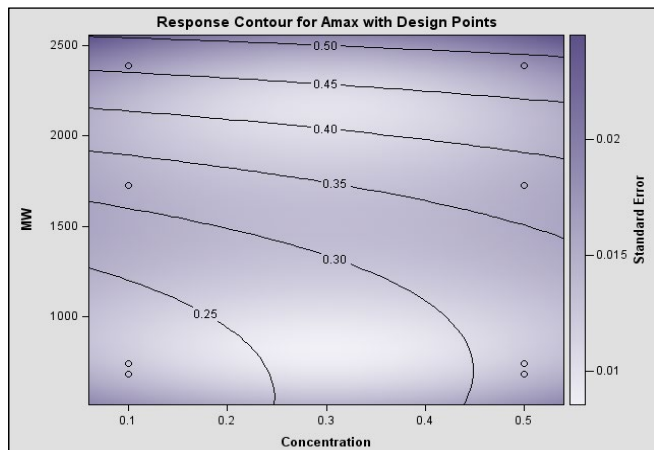


Figure 5: Contour plot for response of Absorbance maxima. MW is expressed in KDa and Concentration is expressed in %

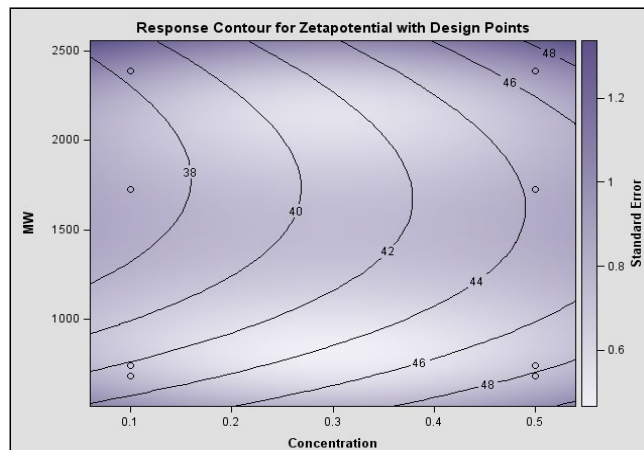


Figure 8: Contour plot for response of Zeta potential (mV). MW is expressed in KDa and Concentration is expressed in %

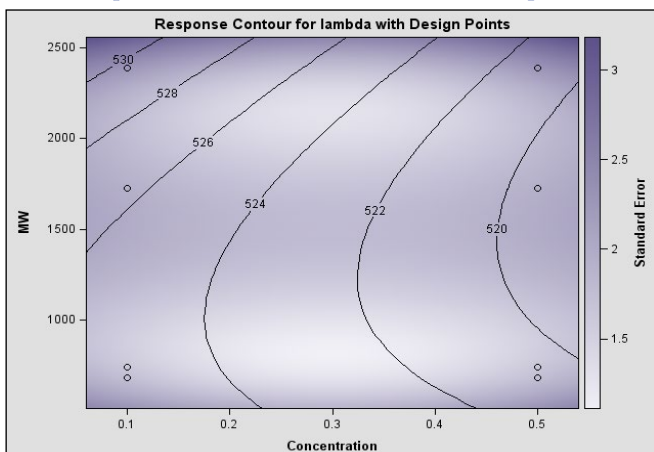


Figure 6: Contour plot for response of λ_{max} (nm). MW is expressed in KDa and Concentration is expressed in %

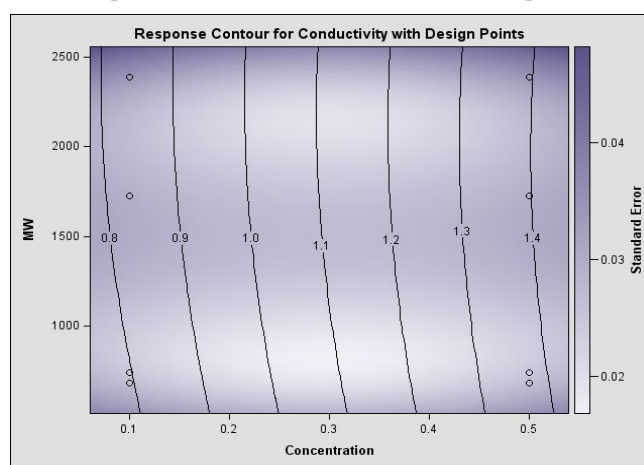


Figure 9: Contour plot for response of Conductivity (mS/cm). MW is expressed in KDa and Concentration is expressed in %

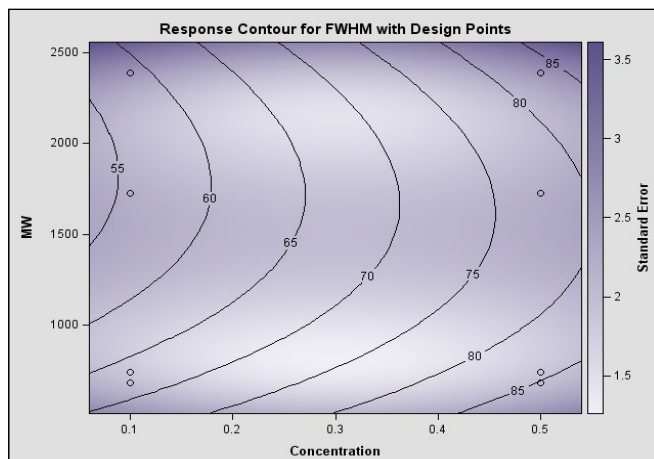


Figure 7: Contour plot for response of full width at half maximum (FWHM). MW is expressed in KDa and Concentration is expressed in %

can be considered as the major factor affecting the FWHM and particle size of nanoparticles. The zeta potential was also found to be increasing with increase in concentration

of chitosan and at lower concentrations, the zeta potential reduces with increase in molecular weight. The samples will have higher conductivity with increase in concentration of chitosan.

3.2. Stability on freezing

In order to study the stability of prepared gold nanocomposites, they were subjected to frozen storage for four days at $-18 \pm 2^\circ\text{C}$. There were changes in visible colour for three samples with lower molecular weight at 0.1% chitosan and the sample prepared with TSC. The visible colour changes are given in Figure 1. The extensive ice crystal growth in nanocomposite solutions causes reduction in the available surface area for particles and will lead to increased aggregation of AuNPs (Mithell et al., 2015). The precipitation of polymer over the crystallised water causes aggregation of AuNPs as a result of this ice crystal formation (Wang et al., 2017). Hence in this study the change in colour of the samples are caused due to the aggregation of particles. In lower molecular weight samples the aggregation

caused the colour to change from light pink to partially colourless. The colour change is more evident in these samples as the concentration of gold nanoparticles formed initially was lower when compared to the higher molecular weight samples. The trisodium citrate has changed the colour from ruby red to complete colourless on freezing. This can be correlated with the negative zeta potential of samples prepared with TSC which shows the instability. The change in the absorption band is given in Figures 2-4. The aggregation of AuNPs cause a shift in absorption band to higher wavelength and the colour changes to blue (Kreibig and Genzel, 1985)

The samples synthesised with higher chitosan concentration have not shown any colour change on freezing. This can be correlated with the higher zeta potential of samples. At lower chitosan concentrations, the charge rendered is small and hence the repulsion is less and this results in higher aggregation. A depression in freezing point is caused by an increase in polymer concentration in nanocomposite solutions and hence there will be a reduction in formation of ice crystals (Cooney et al., 2008). This reduction can cause a reduction in aggregation of the nanoparticles also. The plasmonic peak of nanoparticles have not changed the wavelength of maximum absorbance in any of the samples. The absorbance maxima have reduced in all the samples irrespective of the molecular weight and concentration of chitosan used. In AuNP synthesised with TSC, there was flattening of band at ~520 nm on freezing which shows the changes in nanoparticles formed and thus the change in colour. In this study it was seen that the nanoparticles are stabilised by chitosan when compared to the AuNPs synthesised with sodium citrate.

The reduction in absorbance maxima was higher in lower molecular weight samples at 0.1% chitosan concentration. This is in contrary to the higher zeta potential value of the samples with lower molecular weight chitosan. The initial colour change of gold nanoparticles occur when aggregation of approximately 11 nanoparticles are there (Kim et al., 2008). On use of polyvinyl alcohol as stabilising agent, the molecular weight affects the stability of nanoparticles only at lower concentration (Congdon et al., 2015).

4. CONCLUSION

The synthesis of gold nanoparticles was studied using 1mM gold precursor and chitosan. The molecular weight of chitosan was the major factor affecting the absorption maxima while the Full width at half maximum, particle size, zeta potential and conductivity of the nanoparticles were affected by concentration of chitosan than the molecular weight. The nanoparticles produced using TSC have changed colour to colourless on freezing

and hence can be used as cost effective freeze indicator with lower gold concentrations.

5. ACKNOWLEDGEMENT

The authors would like to acknowledge the Director, ICAR-Central Institute of Fisheries Technology, Cochin for the support given for carrying out the work.

6. REFERENCES

- Akhtar, M.S., Panwar, J., Yun, Y.S., 2013. Biogenic synthesis of metallic nanoparticles by plant extracts. *ACS Sustainable Chemistry & Engineering* 1(6), 591–602.
- Amr, H.H., Shehabeldine, A.M., Omar, M.A., Salem, S.S., 2022. Synthesis of chitosan-based gold nanoparticles: antimicrobial and wound-healing activities. *Polymers*, doi: 10.3390/polym14112293
- Kamaraj, C., Karthi, S., Reegan, A.D., Balasubramani, G., Ramkumar, G., Kalaivani, K., Zahir, A.A., Paramasivam, D., Sengottayan, S.N., Abu, R.M., Islam, T., Malafaia, G., 2022. Green synthesis of gold nanoparticles using *Gracilaria crassa* leaf extract and their ecotoxicological potential: Issues to be considered. *Environmental Research*, doi: 10.1016/j.envres.2022.113711. Epub 2022 Jun 18. PMID: 35728640.
- Cooney, M.J., Lau, C., Windmeisser, M., Liaw, B.Y., Klotzbach, T., Minter, S.D., 2008. Design of chitosan gel pore structure: towards enzyme catalyzed flow-through electrodes. *Journal of Materials Chemistry* 18(6), 667–674.
- Khan, F., Mohammad, S., Mohd, A., Mansoor, A.S., Pieter, M., Ahmad, F., 2022. Green nanotechnology: plant-mediated nanoparticle synthesis and application. *Nanomaterials* 12(4), 673. doi: 10.3390/nano12040673
- Gao, Q., Liu, X., Wang, Z., 2024. *In vitro* and *in vivo* characterization of *Laurus nobilis* loaded chitosan nanoparticles as a potential treatment for gastric cancer using SEM images, PCR and histopathology. *Journal of Biomedical Nanotechnology* 20(3), 494–499.
- Jayakumar, R., Menon, D., Manzoor, K., Nair, S.V., Tamura, H., 2010. Biomedical applications of chitin and chitosan based nanomaterials—a short review. *Carbohydrate Polymers* 82(2), 227–232.
- Keijok, W.J., Pereira, R.H.A., Alvarez, L.A.C., Prado, A.R., da Silva, A.R., Ribeiro, J., Oliveira, Guimarães, M.C.C., 2019. Controlled biosynthesis of gold nanoparticles with *Coffea arabica* using factorial design. *Scientific Reports* 9(1), 16019.
- Kim, T., Lee, C.H., Joo, S.W., Lee, K., 2008. Kinetics of gold nanoparticle aggregation: experiments and modeling. *Journal of Colloid and Interface Science*



- 318(2), 238–243.
- Kimling, J., Maier, M., Okenve, B., Kotaidis, V., Ballot, H., Plech, A., 2006. Turkevich method for gold nanoparticle synthesis revisited. *The Journal of Physical Chemistry B*, 110(32), 15700–15707.
- Kreibig, U., Genzel, L.J.S.S., 1985. Optical absorption of small metallic particles. *Surface Science* 156, 678–700.
- Li, Q., Dunn, E.T., Grandmaison, E.W., Goosen, M.F., 2020. Applications and properties of chitosan. “Applications and properties of chitosan.” In *Applications of Chitin and Chitosan*, 3–29. CRC Press, 2020.
- Merza, K.S., Al-Attabi, H.D., Abbas, Z.M., Yusr, H.A., 2012. Comparative study on methods for preparation of gold nanoparticles. *Green and Sustainable Chemistry* 2(1), 26–28.
- Mihir, R., Mehta, Harshal, P., Mahajan, Amol, U., Hivrle, 2021. Green synthesis of chitosan capped-copper nano biocomposites: synthesis, characterization, and biological activity against plant pathogens. *Journal of Bionanoscience*, doi: 10.1007/S12668-021-00823-8
- Mitchell, D.E., Congdon, T., Rodger, A., Gibson, M.I., 2015. Gold nanoparticle aggregation as a probe of antifreeze (glyco) protein-inspired ice recrystallization inhibition and identification of new IRI active macromolecules. *Scientific Reports* 5(1), 15716.
- Mizutani, T., Ogawa, S., Murai, T., Nameki, H., Yoshida, T., Yagi, S., 2015. *In situ* UV–vis investigation of growth of gold nanoparticles prepared by solution plasma sputtering in NaCl solution. *Applied Surface Science* 354, 397–400.
- Mohan, C.O., Gunasekaran, S., Ravishankar, C.N., 2019. Chitosan-capped gold nanoparticles for indicating temperature abuse in frozen stored products. *NPJ Science of Food* 3(1), 2.
- Najlaa, S., Al-Radadi, 2022. Single-step green synthesis of gold conjugated polyphenol nanoparticle using extracts of Saudi’s myrrh: Their characterization, molecular docking and essential biological applications. *Journal of The Saudi Pharmaceutical Society*, doi: 10.1016/j.jsps.2022.06.028
- Osman, Z., Arof, A.K., 2003. FTIR studies of chitosan acetate based polymer electrolytes. *Electrochimica Acta* 48(8), 993–999.
- RaviKumar, M.N.V., 1999. Chitin and chitosan fibres: a review. (1999) *Bulletin of Materials Science* 22(5), 905.
- Prashanth, K.H., Tharanathan, R.N., 2007. Chitin/chitosan: modifications and their unlimited application potential-an overview. *Trends in Food Science & Technology* 18(3), 117–131.
- Regiel-Futyra, A., Kus-Liskiewicz, M., Sebastian, V., Irusta, S., Arruebo, M., Stochel, G., Kyzioł, A., 2015. Development of noncytotoxic chitosan–gold nanocomposites as efficient antibacterial materials. *ACS Applied Materials & Interfaces* 7(2), 1087–1099.
- Harikrishnan, R., Navaneethan, K., Rajesh, S., 2022. Green synthesis and characterization of bisphosphonate conjugated gold nanoparticle with *cissus quadrangularis* extract to enhance orthodontic anchorage. *International Journal of Health Sciences (IJHS)*, doi: 10.53730/ijhs.v6ns5.11622.
- Dananjaya, S.H.S., Udayangani, R.M.C., Oh., C., Nikapitiya, C., Lee, J., De, Zoysa, M., 2017. Green synthesis, physio-chemical characterization and anti-candidal function of a biocompatible chitosan gold nanocomposite as a promising antifungal therapeutic agent. *RSC Advances*, doi: 10.1039/C6RA26915J
- Sandford, P.A., Zikakis, P.A., Brine, C.J., 1992. *Advances in chitin and chitosan*. Elsevier Applied Science, 516–25.
- Santhoshkumar, J., Rajeshkumar, S., Kumar, S.V., 2017. Phyto-assisted synthesis, characterization and applications of gold nanoparticles—A review. *Biochemistry and Biophysics Reports* 11, 46–57.
- Sreelakshmi, K.R., Mohan, C.O., Anas, K.K., Renjith, R.K., Remya, S., Ashraf, P.M., 2022^a. Synthesis and stability of chitosan gold nanocomposites: Effect of time of heating and concentration of reactant. *International Journal of Food Science & Technology* 57(2), 1333–1339.
- Sreelakshmi, K.R., Mohan, C.O., Remya, S., Tejpal, C.S., Ravishankar, C.N., 2022^b. Intrinsic properties of chitosan on the characteristics of gold nanoparticles and its application as smart packaging device. *Food Science and Technology International*, 10820132221141944.
- Sreelakshmi, K.R., Mohan, C.O., Pillai, D., Rajasree, R., Ravishankar, C.N., 2021^a. Effect of treatment time on synthesis of silver nanoparticles using chitosan and its stability during freezing. *Fishery Technology* 58(4), 210–213.
- Sreelakshmi, K.R., Mohan, C.O., Remya, S., Raj, R., Rajasree, R., Pillai, D., Asokkumar, K., Ravishankar, C.N., 2021^b. Time dependent synthesis of gold nanoparticles using chitosan as reducing agent: a spectroscopic approach. *Indian Journal of Fisheries* 68(2), 112–117.
- Sun, C., Qu, R., Chen, H., Ji, C., Wang, C., Sun, Y., Wang, B., 2008. Degradation behavior of chitosan chains in the ‘green’ synthesis of gold nanoparticles. *Carbohydrate Research* 343(15), 2595–2599.
- Sun, L., Li, J., Cai, J., Zhong, L., Ren, G., Ma, Q., 2017. One pot synthesis of gold nanoparticles using chitosan with varying degree of deacetylation and molecular

- weight. *Carbohydrate Polymers* 178, 105–114.
- Tyagi, R., Kumar, A., Sardar, M., Kumar, S., Gupta, M.N., 1996. Chitosan as an affinity macroligand for precipitation of N-acetyl glucosamine binding proteins/enzymes. *Isolation and Purification* 2(1996), 217–226.
- Wang, Y.C., Lu, L., Gunasekaran, S., 2017. Biopolymer/gold nanoparticles composite plasmonic thermal history indicator to monitor quality and safety of perishable bioproducts. *Biosensors and Bioelectronics* 92, 109–116.
- Zhang, Y., Schwartzberg, A.M., Xu, K., Gu, C., Zhang, J.Z., 2005. Electrical and thermal conductivities of gold and silver nanoparticles in solutions and films and electrical field enhanced Surface-Enhanced Raman Scattering (SERS). In *Physical Chemistry of Interfaces and Nanomaterials IV* 5929, 193–201. SPIE.